Thermodynamic versus kinetic control in self-assembly of zero-, one-, quasi-two-, and two-dimensional metal-organic coordination structures

Tao Lin,[1] Qi Wu,[1] Jun Liu,[2] Ziliang Shi,[1] Pei Nian Liu,[2] and Nian Lin[1]
[1]*Department of Physics, The Hong Kong University of Science and Technology, Clear Water Bay, Hong Kong, China*
[2]*Shanghai Key Laboratory of Functional Materials Chemistry and Institute of Fine Chemicals, East China University of Science and Technology, Meilong Road 130, Shanghai, China*

(Received 3 September 2014; accepted 25 November 2014; published online 2 February 2015)

Four types of metal-organic structures exhibiting specific dimensionality were studied using scanning tunneling microscopy and Monte Carlo simulations. The four structures were self-assembled out of specifically designed molecular building blocks via the same coordination motif on an Au(111) surface. We found that the four structures behaved differently in response to thermal annealing treatments: The two-dimensional structure was under thermodynamic control while the structures of lower dimension were under kinetic control. Monte Carlo simulations revealed that the self-assembly pathways of the four structures are associated with the characteristic features of their specific heat. These findings provide insights into how the dimensionality of supramolecular coordination structures affects their thermodynamic properties. © *2015 AIP Publishing LLC.* [http://dx.doi.org/10.1063/1.4906174]

I. INTRODUCTION

Metal-directed coordination has been used widely to construct extended metal-organic frameworks (MOFs) as well as discrete supramolecular coordination complexes (SCCs) with polygon or polyhedral morphologies.[1–3] Both MOFs and SCCs contain structure units that are defined by directional coordination bonds and specific molecular backbone geometry. Their synthesis conditions, however, are often different. MOF synthesis involves forming strong bonds and therefore often requires elevated temperatures and pressures. SCCs are stabilized by relatively weak bonds and can be synthesized under milder conditions. In SCC synthesis, kinetic intermediates are progressively converted into thermodynamic products. This can pose a problem for complex structures consisting of multiple components. For example, molecular dynamics simulations revealed that increasing the number of components when assembling coordination cages will lead to kinetically trapped intermediate or side products.[4,5] Another difference between MOFs and SCCs is their dimensionality. MOFs range from extended three-dimensional (3D) frameworks to two-dimensional (2D) sheets and one-dimensional (1D) chains, while SSCs are either discrete (0D) polygons or polyhedrons. As dimensionality is critical in determining the thermodynamic properties of a structure, MOFs and SCCs are expected to follow distinctive self-assembly pathways. Understanding the thermodynamic properties of metal-organic structures of different dimensionality may shed light on the self-assembly mechanisms of MOFs and SCCs. An in-depth understanding of a structure's thermodynamic and statistical properties would help to address the recommendation of Samorì *et al.* to advance self-assembly from empirism to determinism.[6]

In this work, we studied the self-assembly of supramolecular coordination structures of different dimensionality subjected to annealing treatments in order to probe their response towards thermodynamic and kinetic controls. Coordination structures can be assembled from metal centers and ligands at interfaces of solid-liquid[7,8] or solid-vacuum[9–11] phases. This approach has generated a large variety of 2D coordination porous networks,[12–14] 1D coordination polymers,[15–18] and relatively few 0D coordination polygons[18–20] on surfaces. In this study, we employed a family of porphyrin derivatives with pyridyl (py) functional groups and a bis-terpyridyl (terpy) compound to construct 2D frameworks, quasi-2D ladders, 1D chains, and 0D polygons on a Au(111) surface. As illustrated in Fig. 1, porphyrin derivatives of **1**, **2**, **3**, or **4** self-assemble with compound **5** via the py-Fe-terpy coordination motif, resulting in a bi-component 0D square (**1**+**5**), 1D chain (**2**+**5**), quasi-2D ladder (**3** + **5**), or 2D framework (**4** + **5**), respectively. These structures are denoted as the target structures, which feature the thermodynamic stable structures of the four systems. We used scanning tunneling microscopy (STM) to resolve the structures formed after annealing treatments at different temperatures. We observed that in addition to the target structures, various kinetically trapped structures had formed. Interestingly, the four bi-component systems behaved differently upon thermal annealing treatments. Using Monte Carlo (MC) simulation,[21–24] we investigated how the dimensionality of the supramolecular structures affects their thermodynamic properties. In particular, the simulations revealed that the structures with different dimensionalities exhibited distinctive specific heat characteristics,[25–27] consistent with the experimental observations. Furthermore, we propose protocols for directing the self-assembly towards the target structures.

II. METHOD

A. Experimental method

Experiments were performed in an ultrahigh-vacuum system (Omicron Nanotechnology) with base pressure below 5 $\times 10^{-10}$ millibars. A single-crystalline Au(111) substrate was

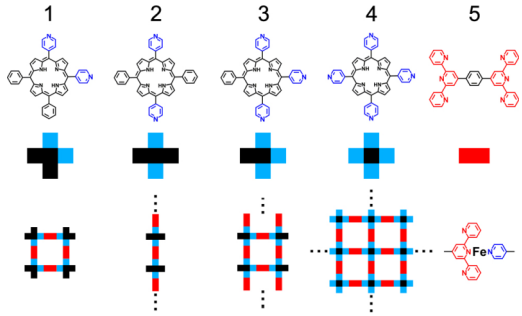

FIG. 1. Top row: molecular ligands used in this study. **1**-**4**: porphyrin derivatives with pyridyl endgroups; **5**: bis-terpyridyl compound. Middle row: schematic representation of the five molecules (py/terpy function is colored in blue/red and phenyl in black). Bottom row: the target structures of the four bi-component systems and py-Fe-terpy coordination motif.

cleaned by Argon-ion sputtering and annealing. The molecules **4** and **5** were purchased from Sigma Aldrich. **1**, **2**, and **3** were synthesized. A molecular beam evaporator was used to thermally evaporate and deposit the molecules onto the Au(111) substrate which was held at room temperature. The evaporation temperatures for **1**–**5** were 610 K, 610 K, 620 K, 660 K, and 550 K, respectively. After depositing the molecules, an electron beam evaporator was used to deposit iron atoms from an iron rod onto the substrate. The STM measurements were performed at 300 K. The data were processed using the WSxM software.[28]

B. Simulation method

A substrate of square lattice with 100×100 lattice sites was used in MC simulations. Porphyrin molecules (molecules **1**, **2**, **3**, and **4**) are crosses that occupy five lattice sites and molecule **5** is a line that occupies three lattice sites. Periodic boundary condition was applied. Initially, porphyrin molecules and **5** were deposited randomly on the substrate lattice at stoichiometric ratio for forming the target structure. Desorption of the molecules from the substrate was not allowed. When a py ligand of a porphyrin molecule encountered a terpy ligand of **5** in a head-to-head configuration, a coordination bond was formed. Since a four-fold substrate was used in the simulation whereas a six-fold substrate was used in the experiment, the simulated patterns were not identical to the experimentally observed ones. The total energy of the system is $U = -nE_b$, where n is the total number of coordination bonds and E_b is the bond energy (we set $E_b = 0.2$ eV). In each MC step, the program randomly chose a molecule and an empty site at which the molecule attempts to jump. The total energies U_{old} and U_{new} of the configurations before and after the attempting were calculated. A probability $P = \min\left(1, e^{\frac{\Delta U}{kT}}\right)$, where $\Delta U = U_{new} - U_{old}$, k is the Boltzmann constant and T is the temperature, is compared with a random number $r \in (0, 1)$. The jumping was accepted if $r < P$ or rejected if $r > P$. If $r = P$, the displacement had a 50% chance of occurring. The simulations ran 10^9 MC steps in order to reach an equilibrium state.

III. RESULTS AND DISCUSSION

A. Experimental results

In the presence of Fe atoms, co-adsorption of one of the porphyrin derivatives (**1**, **2**, **3**, or **4**) and compound **5** on the surface (denoted as **1**-**5**, **2**-**5**, **3**-**5**, or **4**-**5** system, respectively) generated the supramolecular structures shown in Fig. 2. The porphyrin molecules appear as bright dots, presumably due to the metalation of their macrocyclic core,[29,30] while molecule **5** shows a dumbbell shape. Note that in the absence of Fe, none of these supramolecular structures was formed, confirming that the inter-molecular bonds in these structures were py-Fe-terpy coordination bonds.[31] One can see that the target structures were formed in the **2**-**5** and **4**-**5** systems, whereas other structures including zigzag polymeric chains and interconnected ladder segments emerged in the **1**-**5** and **3**-**5** systems, respectively. We reason that the zigzag polymeric chains were kinetically trapped products due to the low mobility of molecular components in the surface-supported self-assembly processes. Thermal annealing has been commonly used to overcome kinetic traps to attain thermodynamic equilibrium structures. We conducted a series of thermal annealing treatments to examine the self-assembly behavior of the four systems at different temperatures.

Fig. 3 displays the structures formed in the four bi-component systems after the series of annealing treatments. At room temperature (300 K without thermal annealing treatment), the **1**-**5** system formed a few squares of very low yield (~1%), while the zigzag chains dominated (Fig. 3(a)); the **2**-**5** system formed short chains up to three porphyrin units long (Fig. 3(d)); the **3**-**5** system formed randomly connected disordered networks (Fig. 3(g)); and the **4**-**5** system formed small domains of 2D networks (Fig. 3(j)). Figs. 3(b) and 3(e) show the structures formed on the samples of the **1**-**5** and **2**-**5** systems after annealing at 400 K for 10 min (all thermal annealing treatments were applied for the same amount of time if not specified otherwise), respectively. Detailed inspection reveals that the yield of the squares in the **1**-**5** system increased to 2% and the chains in the **2**-**5** system became slightly longer. Annealing

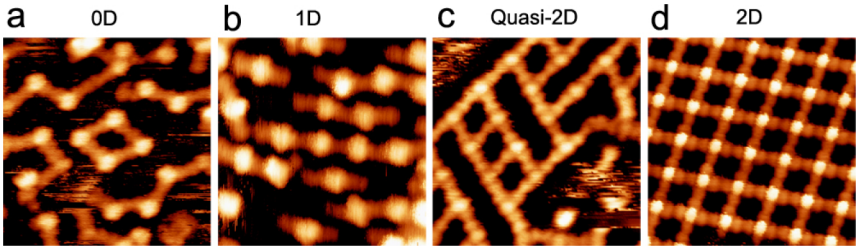

FIG. 2. Representative STM images showing the structures assembled out of Fe and four bi-component systems of **1**-**5** (a), **2**-**5** (b), **3**-**5** (c), and **4**-**5** (d). All images are 20×20 nm^2.

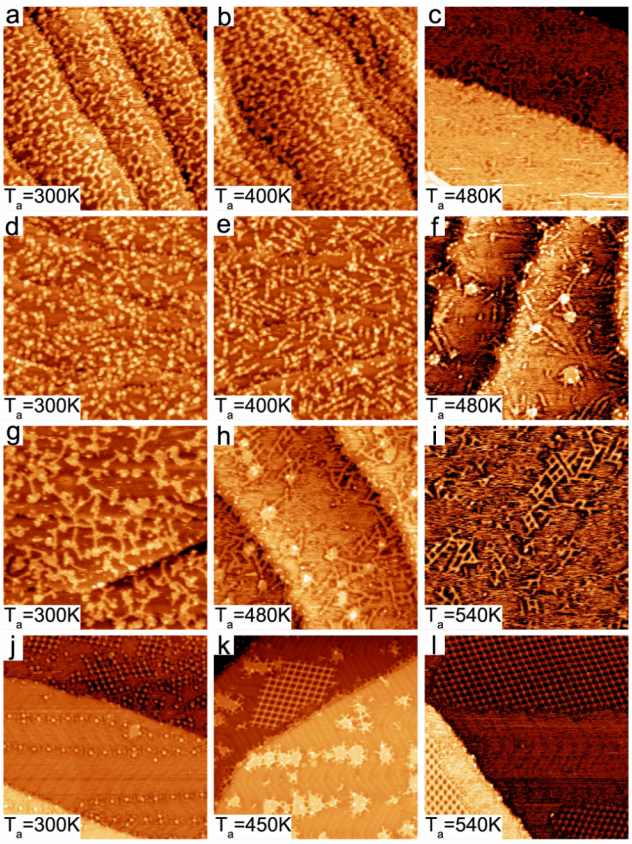

FIG. 3. Representative STM images of the four bi-component systems following a series of thermal annealing treatments. (a)-(c) **1**-**5**. (d)-(f) **2**-**5**. (g)-(i) **3**-**5**. (j)-(l) **4**-**5**. The annealing temperature is indicated in each image. All images are 100×100 nm^2.

for a longer duration (up to 3 h) or at higher temperatures (400 K–450 K) did not change the structures significantly. Further elevating the annealing temperature, however, destroyed the supramolecular structures. As exemplified in Figs. 3(c) and 3(f), after annealing at 480 K, the square or zigzag structures disappeared in the **1**-**5** system and the chain structures in the **2**-**5** system were greatly reduced.

Note that the apparent molecule density shown in Figs. 3(c) and 3(f) is reduced and the STM topographs appear noisy. To find out why, we re-deposited Fe on the two samples at room temperature whereupon structures similar to those shown in Figs. 3(a) and 3(d) emerged. Thus, we conclude that the 480 K annealing did not desorb the molecules from the surface but converted them to a 2D molecular gas, which moved on the surface quickly and could not be resolved by STM but resulted in the noisy STM topographs. During the annealing process, existing supramolecular structures first dissociated into 2D molecular and atomic gases at high temperature. As the samples cooled down, the gas phase molecules should have re-associated into supramolecular structures via py-Fe-terpy coordination, given all components were present on the surface. But, Figs. 3(c) and 3(f) show that after annealing at 480 K, the amount of Fe atoms was significantly reduced. Thus, many molecules could not form coordination bonds but remained in the 2D gas phase. This effect will be discussed later.

Fig. 3(h) shows the structures formed in the **3**-**5** system after 480 K annealing. Short sections of the ladder structure and inter-connected random networks can be seen. Further annealing at 540 K did not generate longer ladder structures but resulted in similar phenomena observed in the **1**-**5** and **2**-**5** systems, namely, reduced molecule densities and noisy STM topographs (Fig. 3(j)). In sharp contrast to the three lower dimensional systems, annealing the **4**-**5** system can significantly improve its structural perfectness. Figs. 3(j), 3(k), and 3(l) reveal that the domains of the 2D networks grew larger and the structural defects were reduced as the annealing temperature rose progressively from room temperature to 450 K and 540 K. No reduction in molecule density was observed after 540 K annealing.

B. MC simulation results

Fig. 4 shows the simulated structures of the four bi-component systems at room temperature (300 K), at a characteristic temperature T_c (T_c will be defined later), and at 20 K below and 20 K above T_c. At room temperature, the **1**-**5** system mainly formed squares (Fig. 4(a)), the **2**-**5** system formed long chains (Fig. 4(e)), the **3**-**5** system formed ladders and inter-connected ladder units (Fig. 4(i)), and the **4**-**5** system formed a large domain of 2D framework (Fig. 4(m)). All bi-component systems generated the target structures, except the **3**-**5** system in which the inter-connected ladder units are comparable in energy to the perfect ladder structure. The simulations did not reproduce the experimental results obtained at room temperature. We attribute this discrepancy to the fact that at room temperature, the self-assembly was kinetically trapped in the experiments and thus the experimentally observed structures were not the thermodynamic equilibrium ones. The MC simulations, however, generated the thermodynamic stable target structures.

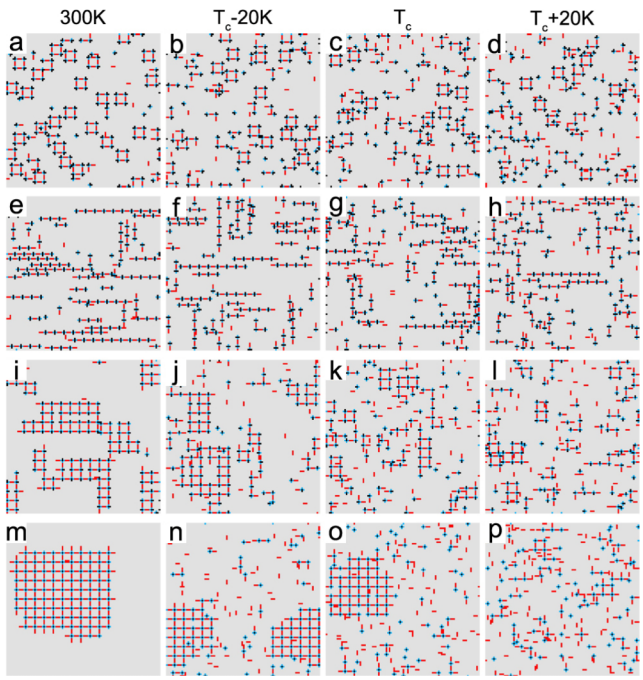

FIG. 4. MC simulated structures of the four bi-component systems formed at different temperatures. (a)-(d) **1**-**5**. (e)-(h) **2**-**5**. (i)-(l) **3**-**5**. (m)-(p) **4**-**5**.

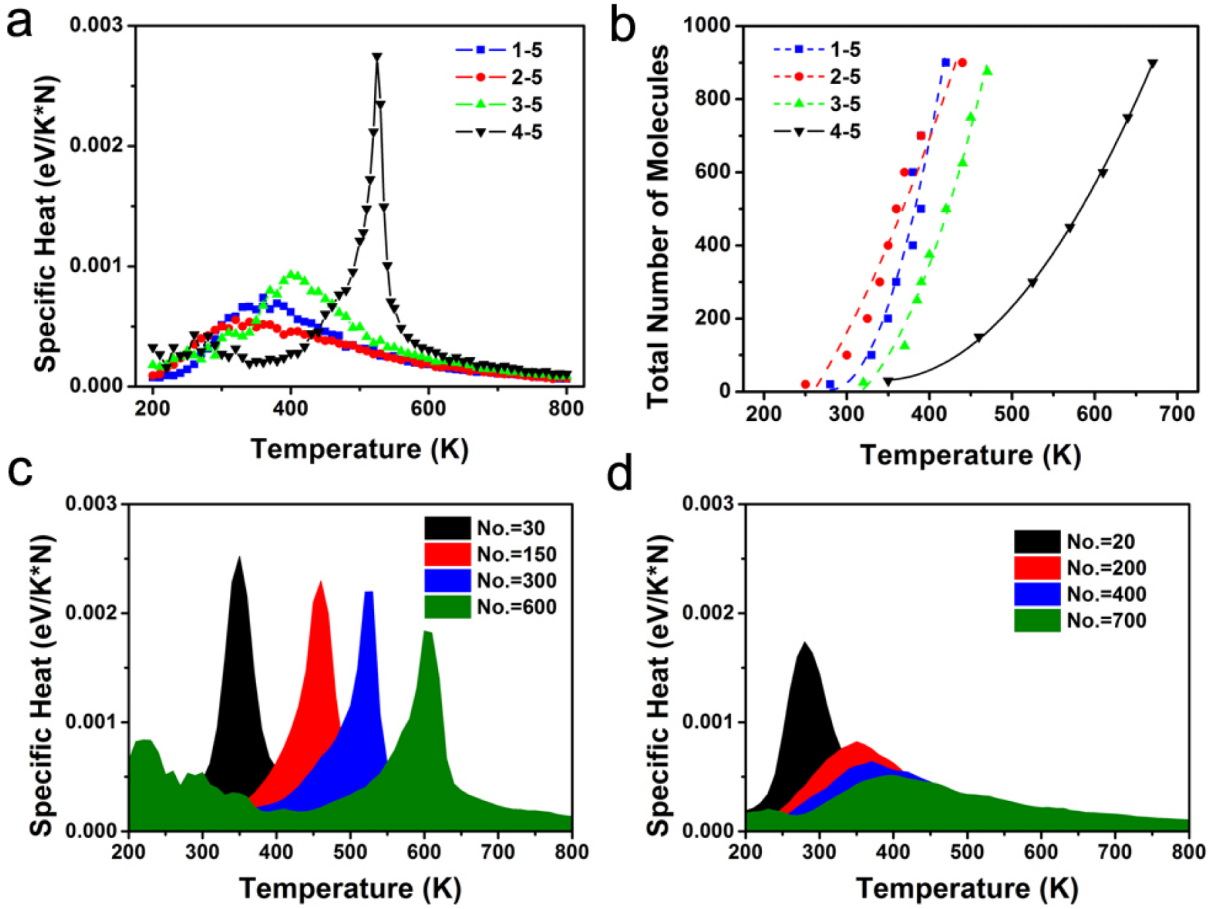

FIG. 5. (a) Simulated specific heats of the four bi-component systems. (b) Phase diagram of the four systems, in which the lines denote T_c. (c) and (d) Simulated specific heats at different molecule densities of **4**-**5** and **1**-**5** systems.

When temperature increased, the supramolecular structures in all four bi-component systems gradually disintegrated into individual molecular components, as shown in Figs. 4(d), 4(h), 4(l), and 4(p). The molecular components were present on the surface as 2D molecular gases. To quantitatively characterize the structural change from the supramolecular phase to the 2D molecular gas phase, we analyzed the specific heat of the four systems. Specific heat was calculated as $c_v = \frac{\langle U^2\rangle - \langle U^2\rangle}{N \times kT^2}$, where U is the total energy of the system and N is the total number of molecules.[32] The simulated specific heat profiles of the four systems are displayed in Fig. 5(a). The specific heat of the **4**-**5** system shows a narrow and salient peak, whereas the specific heats of the **1**-**5**, **2**-**5**, and **3**-**5** systems exhibit a broad hill-like profile with a relatively small maximum. The specific heat maxima (defined as T_c) are 350 K, 325 K, 400 K, and 525 K for the **1**-**5**, **2**-**5**, **3**-**5**, and **4**-**5** systems, respectively. T_c of the **2**-**5**, **3**-**5**, and **4**-**5** systems scales nearly linearly with the number of bonds per molecule (both components are counted) in the target structures, which are 1, 1.2, and 1.6 in the chain, ladder, and 2D framework structures, respectively. This relationship implies that T_c reflects the binding energy per molecule in each structure. The **1**-**5** system has a higher T_c than the **2**-**5** system (350 K vs. 325 K) because in the **1**-**5** system the molecules may form finite-long zigzag chains, which presumably contribute to a specific heat similar to that of the **2**-**5** system or they may form squares or larger closed loops. There is one bond per molecule in the closed loops but less than one in the finite-long chains. The overall contribution of the two types of structures formed in the **1**-**5** system thus leads to a T_c higher than that of the **2**-**5** system.

The structural change from a supramolecular phase below T_c to a 2D gas phase above T_c suggests that T_c is associated with a phase change. The sharp specific heat of the **4**-**5** system may be attributed to a first-order phase transition from 2D solid to 2D gas, with T_c being the critical transition temperature.[33,34] In contrast, the broad hill-like specific heat profiles of the three lower dimensional structures make defining a phase transition critical temperature non-trivial. Careful inspection of Fig. 4 reveals that the **4**-**5** system underwent an abrupt structural change at T_c, i.e., the 2D networks were almost entirely dissolved into gas phase at $T_c + 20$ K, whereas the **1**-**5** and **2**-**5** systems underwent a much smoother transition since the structural change between $T_c - 20$ K and $T_c + 20$ K is less significant. The behavior of the **3**-**5** system was somewhere in between. The simulated specific heat and the structural change of the four systems are consistent with the general understanding that confining a piece of material by restricting some of its dimensions suppresses the phase transition and thus smoothens the peak feature in specific heat. For example, phase transitions were found to be sudden in the bulk of helium but gradual when He atoms were confined in thin films, in narrow channels, or in microscopic boxes.[35]

C. Discussion

The simulations provide insights for understanding the experimental data. Since the molecules or atoms involved in the four systems possess almost identical surface mobility and coordination bond strength, we attribute the different thermodynamic behaviors of the four systems to the dimensionality of the supramolecular structures formed wherein. In an annealing process, the sample temperature is raised first so that the formed coordination bonds may be broken, and the freed molecules and atoms gain sufficient energy to move on the surface. The former process allows reversibility in self-assembly for forming thermodynamically stable structures. The latter process dictates self-assembly kinetics. Interplay of thermodynamics and kinetics determines the self-assembly pathway. When the sample cools down to approximately T_c, the molecular components begin to form supramolecular structures. For a system featuring a specific heat with a broader hill-like profile, transition from the 2D gas phase to the supramolecular phase takes place in a wide temperature window, in which various kinetically trapped intermediate structures may form, and thus formation of the target structures requires sufficient long period. Annealing the sample to a higher temperature does not facilitate the formation of the target structures for such systems. Instead, a prolonged annealing at a moderate temperature may yield more target structures. This mechanism explains the experimental results that thermal annealing to higher temperatures could not increase the yield of the 0D, 1D, and quasi-2D target structures.

In addition to the shape of the specific heat profile, T_c is also an important parameter to be considered. For a system with low T_c, the assembly is a slow process because of the low mobility of the molecules or atoms. Meanwhile, the formed bonds do not break easily and thus reversibility is reduced. Moreover, only the molecules at the boundary of the domains effectively dissociate and re-associate. All these effects hinder error correction and reduce the assembly rate of the target structures. Therefore, the low kinetics inherently prohibits a system with a broader hill-like specific heat profile peaked at low T_c to form the target structures. To overcome the kinetic limitation discussed herein, a system must have a sharp specific heat peak at high temperature. Such a system may generate high-yield target structures through thermal annealing.

A low T_c introduces another effect in our systems: loss of Fe atoms after high-temperature annealing. At a high temperature, the py-Fe-terpy coordination bonds are dissociated and the Fe atoms are present as a 2D atomic gas on the surface. While the sample is cooling down, the Fe atoms may re-associate the molecular components into the supramolecular structures, or they may participate in other processes including nucleation into Fe clusters (such Fe clusters can be found in Fig. 3(f)) or be adsorbed at steps or defects on the surface. If these competing processes occur at temperatures above T_c, there may not be enough free Fe atoms available for forming coordination bonds at T_c. Our experimental observation that the apparent molecular density was reduced after annealing the **1**-**5**, **2**-**5**, and **3**-**5** systems at high temperature suggests that this effect took place in these systems. To achieve a high yield of the target structure in these systems, assembly should take place at T_c for a long duration while slowly adding Fe atoms to the pre-deposited molecules on the surface.

Finally, we carried out a series of simulations to explore the effects of molecule density on phase transition. From these simulations, we constructed a phase diagram as shown in Fig. 5(b), in which the solid curve indicates the abrupt phase transition that occurred in the **4**-**5** system and the dotted curves indicate the smooth transition in the **1**-**5**, **2**-**5**, and **3**-**5** systems. In all four systems, the transition shifted toward higher temperatures as the molecule density increased. The specific heat profile of the **4**-**5** system remains sharp at higher densities as shown in Fig. 5(c), implying that large area perfect 2D networks can be assembled simply by elevating the annealing temperature.[30] However, as shown in Fig. 5(d), the **1**-**5** system displays a broader specific heat profile at higher molecule densities when T_c is higher. Hence, for this system, neither a low nor a high molecule density meets the criteria for a thermodynamically controlled process. We conclude that self-assembly of the 0D target structures is intrinsically kinetically controlled. To produce a sharp specific heat profile at a high temperature, stronger coordination bonds and a low molecule density must be applied.

IV. CONCLUSION

Using STM and MC simulation, we have compared and analyzed the thermodynamic characteristics of four bi-component coordination systems assembled on Au(111). It turns out that only the 2D target structure can be formed through thermal annealing treatment but the structures of lower dimensionality (0D, 1D, and quasi-2D) are more vulnerable to kinetic traps as a result of their broader-shaped and low-temperature specific heat maxima. Based on these findings, we proposed self-assembly protocols for forming 0D structures in high yields.

ACKNOWLEDGMENTS

This work was financially supported by Hong Kong Research Grants Council (Project No. 602712).

[1]T. R. Cook, Y. R. Zheng, and P. J. Stang, Chem. Rev. **113**, 734 (2013).
[2]H. Furukawa, K. E. Cordova, M. O'Keeffe, and O. M. Yaghi, Science **341**, 1230444 (2013).
[3]R. Chakrabarty, P. S. Mukherjee, and P. J. Stang, Chem. Rev. **111**, 6810 (2011).
[4]M. Yoneya, T. Yamaguchi, S. Sato, and M. Fujita, J. Am. Chem. Soc. **134**, 14401 (2012).
[5]M. Yoneya, S. Tsuzuki, T. Yamaguchi, S. Sato, and M. Fujita, ACS Nano **8**, 1290 (2014).
[6]C. A. Palma, M. Cecchini, and P. Samorì, Chem. Soc. Rev. **41**, 3713 (2012).
[7]H.-M. Zhang, W. Zhao, Z.-X. Xie, L.-S. Long, B.-W. Mao, X. Xu, and L.-S. Zheng, J. Phys. Chem. C **111**, 7570 (2007).
[8]S. Yoshimoto, Y. Ono, K. Nishiyama, and I. Taniguchi, Phys. Chem. Chem. Phys. **12**, 14442 (2010).
[9]J. V. Barth, Annu. Rev. Phys. Chem. **58**, 375 (2007).
[10]N. Lin, S. Stepanow, M. Ruben, and J. V. Barth, Top. Curr. Chem. **287**, 1 (2009).
[11]S. Stepanow, N. Lin, and J. V. Barth, J. Phys.: Condens. Matter **20**, 184002 (2008).
[12]A. Dmitriev, H. Spillmann, N. Lin, J. V. Barth, and K. Kern, Angew. Chem., Int. Ed. **42**, 2670 (2003).
[13]D. Kühne, F. Klappenberger, R. Decker, U. Schlickum, H. Brune, S. Klyatskaya, M. Ruben, and J. V. Barth, J. Am. Chem. Soc. **131**, 3881 (2009).

[14]H. Liang, Y. He, Y. Ye, X. Xu, F. Cheng, W. Sun, X. Shao, Y. Wang, J. Li, and K. Wu, Coord. Chem. Rev. **253**, 2959 (2009).
[15]T. Classen, G. Fratesi, G. Costantini, S. Fabris, F. L. Stadler, C. Kim, S. De Gironcoli, S. Baroni, and K. Kern, Angew. Chem., Int. Ed. **44**, 6142 (2005).
[16]S. L. Tait, A. Langner, N. Lin, S. Stepanow, C. Rajadurai, M. Ruben, and K. Kern, J. Phys. Chem. C **111**, 10982 (2007).
[17]D. Heim, D. Écija, K. Seutert, W. Auwärter, C. Aurisicchio, C. Fabbro, D. Bonifazi, and J. V. Barth, J. Am. Chem. Soc. **132**, 6783 (2010).
[18]L. A. Fendt, M. Stöhr, N. Wintjes, M. Enache, T. A. Jung, and F. Diederich, Chem. - Eur. J. **15**, 11139 (2009).
[19]D. Heim, K. Seufert, W. Auwärter, C. Aurisicchio, C. Fabbro, D. Bonifazi, and J. V. Barth, Nano Lett. **10**, 122 (2010).
[20]T. Lin, X. S. Shang, P. N. Liu, and N. Lin, J. Phys. Chem. C **117**, 23027 (2013).
[21]A. Ciesielski, P. J. Szabelski, W. Rżysko, A. Cadeddu, T. R. Cook, P. J. Stang, and P. Samori, J. Am. Chem. Soc. **135**, 6942 (2013).
[22]P. Szabelski and S. De Feyter, CrystEngComm **13**, 5542 (2011).
[23]S. Fortuna, D. L. Cheung, and A. Troisi, J. Phys. Chem. B **114**, 1849 (2010).
[24]T. J. Roussel and L. F. Vega, J. Chem. Theory Comput. **9**, 2161 (2013).
[25]T. Misiunas and E. E. Tornau, J. Phys. Chem. B **116**, 2472 (2012).
[26]U. K. Weber, V. M. Burlakov, L. M. A. Perdigao, R. H. J. Fawcett, P. H. Beton, N. R. Champness, J. H. Jefferson, G. A. D. Briggs, and D. G. Pettifor, Phys. Rev. Lett. **100**, 156101 (2008).
[27]A. Ibenskas and E. E. Tornau, Phys. Rev. E **86**, 051118 (2012).
[28]I. Horcas, R. Fernández, J. M. Gómez-Rodríguez, J. Colchero, J. Gómez-Herrero, and A. M. Baro, Rev. Sci. Instrum. **78**, 013705 (2007).
[29]J. M. Gottfried and H. Marbach, Z. Phys. Chem. **223**, 53 (2009).
[30]Y. Li, J. Xiao, T. E. Shubina, M. Chen, Z. Shi, M. Schmid, H.-P. Steinrück, J. M. Gottfried, and N. Lin, J. Am. Chem. Soc. **134**, 6401 (2012).
[31]Z. Shi and N. Lin, J. Am. Chem. Soc. **132**, 10756 (2010).
[32]I. G. Johnston, A. A. Louis, and J. P. K. Doye, J. Phys.: Condens. Matter **22**, 104101 (2010).
[33]B. Kuchta and R. D. Etters, Phys. Rev. B **54**, 12057 (1996).
[34]K. Wierschem and E. Manousakis, Phys. Rev. B **83**, 214108 (2011).
[35]M. O. Kimball, K. P. Mooney, and F. M. Gasparini, Phys. Rev. Lett. **92**, 115301 (2004).